

Flavor Non-universal Vector Leptoquark Imprints in $K \rightarrow \pi\nu\bar{\nu}$ and $\Delta F = 2$ Transitions

Òscar L. Crosas,^{1,*} Gino Isidori,^{1,†} Javier M. Lizana,^{1,‡} Nudžeim Selimović,^{1,§} and Ben A. Stefanek^{1,¶}

¹*Physik-Institut, Universität Zürich, CH-8057 Zürich, Switzerland*

We analyze $K \rightarrow \pi\nu\bar{\nu}$ rates in a model with a TeV-scale leptoquark addressing B -meson anomalies, based on the flavor non-universal 4321 gauge group featuring third-generation quark-lepton unification. We show that, together with the tight bounds imposed by $\Delta F = 2$ amplitudes, the present measurement of $\mathcal{B}(K^+ \rightarrow \pi^+\nu\bar{\nu})$ already provides a non-trivial constraint on the model parameter space. In the minimal version of the model, the deviations from the Standard Model in $\mathcal{B}(K^+ \rightarrow \pi^+\nu\bar{\nu})$ are predicted to be in close correlation with non-standard effects in the Lepton Flavor Universality ratios R_D and R_{D^*} . With the help of future data, these correlations can provide a decisive test of the model.

I. INTRODUCTION

The anomalies in neutral-current [1–4] and charged-current [5–10] B -meson decays have triggered a renewed interest in precision tests of semi-leptonic processes, and in particular in transitions involving third-generation fermions. In this general context, $K \rightarrow \pi\nu\bar{\nu}$ decays play a very special role. First, these processes are among the very few flavor-changing transitions involving light quarks ($s \rightarrow d$) that we are able to compute precisely within the Standard Model (SM) (see [11] for state-of-the-art predictions). Second, they are extremely suppressed within the SM due to its approximate accidental symmetries, making them a particularly sensitive probe of possible new physics (NP). Third, these processes uniquely probe the couplings of light quarks to third-generation leptons via tau neutrinos in the final state. Last but not least, the NA62 experiment at CERN is now sensitive enough to test the SM prediction for the branching ratio of the charged kaon decay mode, $\mathcal{B}(K^+ \rightarrow \pi^+\nu\bar{\nu})$ [12].

The connection between $K \rightarrow \pi\nu\bar{\nu}$ and the B anomalies has been explored in a series of recent papers, both adopting a general EFT approach [13, 14], as well as in specific new physics models [15, 16]. From these previous studies, it emerges quite clearly that an $O(10\%)$ deviation from the SM in the Lepton Flavor Universality (LFU) ratios $R_{D^{(*)}}$ naturally implies $O(1)$ deviations from the SM in $\mathcal{B}(K^+ \rightarrow \pi^+\nu\bar{\nu})$. However, the precise size of the effect is rather model dependent.

In this paper, we address the precise connection between $R_{D^{(*)}}$ and $\mathcal{B}(K^+ \rightarrow \pi^+\nu\bar{\nu})$ in the framework of a particularly motivated class of SM extensions. We focus on models where the B anomalies are described by the exchange of a TeV-scale vector leptoquark (LQ) [17–21] arising from the spontaneous symmetry breaking of

the flavor non-universal gauge group $SU(4)_h \times SU(3)_l \times SU(2)_L \times U(1)_X$ down to the SM [22–26]. In these so-called non-universal 4321 models, color is embedded as the diagonal subgroup of $SU(4)_h \times SU(3)_l$ [22], where the labels h (heavy) and l (light) indicate the flavor non-universal charge assignment of the SM fermions under this part of the gauge group. This setup is particularly appealing as it results in quark-lepton unification à la Pati-Salam [27] for third-generation fermions, an accidental approximate $U(2)^5$ flavor symmetry, and a U_1 vector LQ that is automatically dominantly coupled to the third family [23–26]. As recently shown in [28, 29] this setup can arise from a higher dimensional (or multi-scale) construction addressing both the origin of the SM flavor hierarchies [23, 30–32] as well as the electroweak (EW) hierarchy problem [33, 34], with an intrinsic theoretical interest that goes beyond the B anomalies.

This ambitious class of models contains a sizeable number of new fields compared to the SM. In particular, in addition to the LQ, two neutral massive vectors (an octet and a singlet of color), as well as one or more families of vector-like (VL) fermions are necessarily present: these exotic (heavy) fermions are required in order to generate mixing between the light and third generations, which is needed both in the Yukawa sector as well as in the couplings to the new massive gauge fields. Despite the presence of new exotic fields, a large fraction of the model parameters are fixed by observable quantities. These include the B anomalies, a series of tight constraints from various low-energy precision tests, and the elements of the Cabibbo-Kobayashi-Maskawa (CKM) matrix, which are now calculable in the model in terms of more fundamental parameters. This results in a highly predictive framework, at least in the minimal version of the model with only one family of VL fermions, which is what we consider in this paper. As we show, the tight constraints from $\Delta F = 2$ observables (in particular ϵ_K and CP violation in $D-\bar{D}$ mixing) imply a well-defined structure for the couplings of the light quarks to the new heavy states that, in turn, leads to a clear correlation between $R_{D^{(*)}}$ and $\mathcal{B}(K^+ \rightarrow \pi^+\nu\bar{\nu})$.

* olaracrosas@student.ethz.ch

† isidori@physik.uzh.ch

‡ jlizana@physik.uzh.ch

§ nudzeim@physik.uzh.ch

¶ bestef@physik.uzh.ch

The paper is organised as follows. In Section II we introduce the model. In Section III, we analyze $\Delta F = 2$ observables and determine the range of the parameters controlling flavor mixing in the light-quark sector. Using these results, in Section IV we analyze the predictions for $\mathcal{B}(K^+ \rightarrow \pi^+ \nu \bar{\nu})$. The results are summarized in the conclusions. The appendices contain: A) a detailed analysis of the flavor structure of the model, including the computation of the CKM matrix; B) a discussion about the inclusion of additional VL fermions charged under $SU(3)_l$; C) expressions relevant to estimate $R_{D^{(*)}}$; D) complete results for the Wilson coefficients (both tree- and one-loop contributions) for the effective operators relevant to $\Delta F = 2$ and $K \rightarrow \pi \nu \bar{\nu}$ observables.

II. THE MODEL

The model we consider is based on the gauge group $\mathcal{G}_{4321} = SU(4)_h \times SU(3)_l \times SU(2)_L \times U(1)_X$, where color is the diagonal subgroup of $SU(4)_h \times SU(3)_l$ and the flavor-universal group $SU(2)_L$ acts as in the SM. The $U(1)_X$ group acts as the SM hypercharge on the first two families, while for the third family $Y = X + \sqrt{2/3} T_4^{15}$, where $T_4^{15} = \frac{1}{2\sqrt{6}} \text{diag}(1, 1, 1, -3)$ is a generator of $SU(4)_h$. The matter content is reported in Table I. In the absence of mixing, the three $SU(4)_h$ multiplets ψ_L and ψ_R^\pm can be identified with the SM third-generation fermions (with the addition of a right-handed neutrino). The only exotic fermion is a single VL fermion ($\chi_{L,R}$), where both chiralities have the same gauge quantum numbers as the chiral field ψ_L .

The massive gauge bosons resulting from the spontaneous symmetry breaking (SSB) $4321 \rightarrow \text{SM}$ transform under the SM gauge group as $U_1 \sim (\mathbf{3}, \mathbf{1}, \mathbf{2}/3)$, $G' \sim (\mathbf{8}, \mathbf{1}, \mathbf{0})$ and $Z' \sim (\mathbf{1}, \mathbf{1}, \mathbf{0})$. This SSB occurs at the TeV scale via the vacuum expectation values of two scalar fields transforming in the anti-fundamental of $SU(4)$, Ω_1 and Ω_3 , which are singlets and triplets under $SU(3)_l$, respectively. Let us denote the four gauge couplings of \mathcal{G}_{4321} as g_i ($i = 1, \dots, 4$).¹ In terms of the mixing angles $\tan^2 \theta_3 = g_3^2/g_4^2$ and $\tan^2 \theta_1 = 2g_1^2/3g_4^2$, the gauge boson masses read

$$m_{U_1} = \frac{g_4 f_{U_1}}{2}, \quad m_{Z', G'} = \frac{m_{U_1}}{\cos \theta_{1,3}} \frac{f_{Z', G'}}{f_{U_1}}, \quad (1)$$

where $f_{U_1}^2 = \omega_1^2 + \omega_3^2$, $f_{Z'}^2 = 3\omega_1^2/2 + \omega_3^2/2$, $f_{G'}^2 = 2\omega_3^2$, and $\omega_{1,3}$ are the $\Omega_{1,3}$ vacuum expectation values. Note that in the custodial $SU(4)_V$ limit $\omega_3 = \omega_1$, all masses are approximately degenerate in the phenomenological limit $g_{1,3} \ll g_4$. More details on the model can be found in [26].

Field	$SU(4)_h$	$SU(3)_l$	$SU(2)_L$	$U(1)_X$
q_L^i	1	3	2	1/6
u_R^i	1	3	1	2/3
d_R^i	1	3	1	-1/3
ℓ_L^i	1	1	2	-1/2
e_R^i	1	1	1	-1
ψ_L	4	1	2	0
ψ_R^\pm	4	1	1	$\pm 1/2$
$\chi_{L,R}$	4	1	2	0
H	1	1	2	1/2
Ω_1	$\bar{\mathbf{4}}$	1	1	-1/2
Ω_3	$\bar{\mathbf{4}}$	3	1	1/6

TABLE I. Minimal matter-field content of the model ($i = 1, 2$). Fields added to the SM matter content are shown in grey.

After the TeV-scale SSB, a mass mixing is induced between chiral and VL fermions. Let us define $\Psi_q'^\top = (q_L^1 \ q_L^2 \ q_L^3 \ Q_L)$ and similarly for the left-handed (LH) leptons. Here, Q_L denotes the LH quark component of the VL field and the prime superscript indicates we are in the interaction (or gauge-eigenstate) basis and not in the mass-eigenstate basis. The mass mixing can be written as

$$-\mathcal{L} \supset \bar{\Psi}_q' \mathbf{M}_q Q_R + \bar{\Psi}_\ell' \mathbf{M}_\ell L_R + \text{h.c.}, \quad (2)$$

and, without loss of generality, we can decompose the mass matrices as

$$\begin{aligned} \mathbf{M}_q &= \mathbf{W}_q^\dagger \mathbf{O}_q^\dagger (0 \ 0 \ 0 \ m_Q)^\top, \\ \mathbf{M}_\ell &= \mathbf{W}_\ell^\dagger \mathbf{O}_\ell^\dagger (0 \ 0 \ 0 \ m_L)^\top, \end{aligned} \quad (3)$$

where m_Q and m_L are TeV-scale masses. The 4×4 unitary rotation matrices can be parameterized as

$$\mathbf{O}_{q,\ell} = \begin{pmatrix} 1 & 0 & 0 & 0 \\ 0 & c_{q,\ell} & 0 & -s_{q,\ell} \\ 0 & 0 & 1 & 0 \\ 0 & s_{q,\ell} & 0 & c_{q,\ell} \end{pmatrix}, \quad \mathbf{W}_{q,\ell} = \begin{pmatrix} \mathbb{1}_{2 \times 2} & 0_{2 \times 2} \\ 0_{2 \times 2} & W_{q,\ell} \end{pmatrix}, \quad (4)$$

where $W_{q,\ell}$ are 2×2 unitary matrices and throughout the paper we adopt the notation $s_{q,\ell} \equiv \sin \theta_{q,\ell}$ and $c_{q,\ell} \equiv \cos \theta_{q,\ell}$. We can move to the VL fermion mass basis (where three chiral fermions species remain massless until EW symmetry breaking) by redefining the LH quark and lepton fields as $\Psi_{q,\ell}' \rightarrow \mathbf{W}_{q,\ell}^\dagger \mathbf{O}_{q,\ell}^\dagger \Psi_{q,\ell}$. In this basis, the interactions of LH fermions with the massive gauge bosons read

$$\mathcal{L}_{U_1} \supset \frac{g_4}{\sqrt{2}} U_1^\mu (\bar{\Psi}_q \beta_L \gamma_\mu \Psi_\ell), \quad (5)$$

$$\mathcal{L}_{G'} \supset g_4 \frac{g_c}{g_3} G_\mu'^a (\bar{\Psi}_q \kappa_q \gamma^\mu T^a \Psi_q), \quad (6)$$

$$\mathcal{L}_{Z'} \supset \frac{g_4}{2\sqrt{6}} \frac{g_Y}{g_1} Z_\mu' [(\bar{\Psi}_q \xi_q \gamma^\mu \Psi_q) - 3(\bar{\Psi}_\ell \xi_\ell \gamma^\mu \Psi_\ell)], \quad (7)$$

¹ In terms of the g_i , the SM gauge couplings for color and hypercharge are $g_c = g_3 \cos \theta_3$ and $g_Y = g_1 \cos \theta_1$.

where, defining $\epsilon_3 = g_3^2/g_4^2$, $\epsilon_1 = 2g_1^2/3g_4^2$, the couplings are given as

$$\kappa_q = \mathbf{O}_q \kappa'_q \mathbf{O}_q^\dagger, \quad \kappa'_q = \text{diag}(-\epsilon_3, -\epsilon_3, 1, 1), \quad (8)$$

$$\xi_q = \mathbf{O}_q \xi'_q \mathbf{O}_q^\dagger, \quad \xi'_q = \text{diag}(-\epsilon_1, -\epsilon_1, 1, 1), \quad (9)$$

$$\xi_\ell = \mathbf{O}_\ell \xi'_\ell \mathbf{O}_\ell^\dagger, \quad \xi'_\ell = \text{diag}(-\epsilon_1, -\epsilon_1, 1, 1), \quad (10)$$

and

$$\beta_L = \mathbf{O}_q \mathbf{W} \beta'_L \mathbf{O}_\ell^\dagger, \quad \mathbf{W} = \begin{pmatrix} \mathbb{1}_{2 \times 2} & 0_{2 \times 2} \\ 0_{2 \times 2} & W \end{pmatrix}, \quad (11)$$

with $\beta'_L = \text{diag}(0, 0, 1, 1)$.

The matrix $W = W_q W_\ell^\dagger$ can always be written as a real, orthogonal 2×2 matrix by re-phasing q_L^3 , ℓ_L^3 , and the LH VL fermions. We parameterize it by an angle θ_χ :

$$W = \begin{pmatrix} c_\chi & s_\chi \\ -s_\chi & c_\chi \end{pmatrix}. \quad (12)$$

A non-trivial W -matrix (i.e. $s_\chi \neq 0$) arises from the difference between the quark and lepton mass matrices in (2), in the sub-sector of the $SU(4)$ -charged fermions [26]. It can be generated by including a scalar field Ω_{15} , transforming as a $(\mathbf{15}, \mathbf{1}, \mathbf{1}, 0)$ of \mathcal{G}_{4321} , which takes a vacuum expectation value ω_{15} along the T_4^{15} generator. This would also shift the mass of the U_1 , modifying the $f_{U_1}^2$ appearing in (1) to $f_{U_1}^2 = \omega_1^2 + \omega_3^2 + 4/3\omega_{15}^2$. Note that the re-phasing making W real results in a phase appearing in the LQ coupling to the right-handed (RH) VL fermions.

A. Yukawa Couplings

We are now ready to analyze the structure of the Yukawa couplings, i.e. the couplings of the four families of $SU(2)_L$ charged fields, the three right-handed chiral fermions, and the Higgs field. Defining $\Psi_u^\dagger = (u_R^1 \ u_R^2 \ u_R^3)$, $\Psi_d^\dagger = (d_R^1 \ d_R^2 \ d_R^3)$, $\Psi_e^\dagger = (e_R^1 \ e_R^2 \ e_R^3)$, the Yukawa couplings in the VL fermion mass basis can be written as

$$-\mathcal{L} \supset \bar{\Psi}_q \mathbf{Y}_u \tilde{H} \Psi_u + \bar{\Psi}_q \mathbf{Y}_d H \Psi_d + \bar{\Psi}_\ell \mathbf{Y}_e H \Psi_e + \text{h.c.}, \quad (13)$$

where $\mathbf{Y}_{u,d,e}$ are 4×3 matrices that can be decomposed as

$$\mathbf{Y}_u = \mathbf{O}_q \begin{pmatrix} U_u^\dagger \hat{Y}_u & \vec{n}_u \\ 0 & y_t \\ 0 & y_t x_t e^{i\varphi_t} \end{pmatrix}, \quad (14)$$

$$\mathbf{Y}_d = \mathbf{O}_q \begin{pmatrix} U_d^\dagger \hat{Y}_d & \vec{n}_d \\ 0 & y_b \\ 0 & y_b x_b e^{i\varphi_b} \end{pmatrix}, \quad (15)$$

$$\mathbf{Y}_e = \mathbf{O}_\ell \mathbf{W}^\dagger \begin{pmatrix} U_e^\dagger \hat{Y}_e & \vec{n}_e \\ 0 & y_b \\ 0 & y_b x_b e^{i\varphi_b} \end{pmatrix}. \quad (16)$$

The overall factors \mathbf{O}_q and $\mathbf{O}_\ell \mathbf{W}^\dagger$ are the results of the rotation from the interaction basis to the VL fermion mass basis, and take into account a global re-definition of both quark and lepton Yukawa of the type $\mathbf{Y}' \rightarrow \mathbf{W}_q^\dagger \mathbf{Y}$, such that the full \mathbf{W} matrix appears only in the lepton sector. As far as the other terms appearing in (14)–(16) are concerned:

- The hatted Yukawas $\hat{Y}_{u,d,e}$ are real, diagonal 2×2 matrices, and $U_{u,d,e}$ are 2×2 unitary matrices with a non-trivial phase each (after field redefinitions). These terms, which control the 2×2 light-family masses (hence the smallest eigenvalues in $\mathbf{Y}_{u,d,e}$) are SM-type Yukawa couplings among the chiral fields not charged under $SU(4)$.
- The entries $y_{t,b}$ and $x_{t,b} e^{i\varphi_{t,b}}$ control the couplings among the $SU(4)$ charged states, i.e. the third-generation Yukawa couplings ($y_{t,b}$) and the Yukawa couplings of the VL fermion to the RH third-generation chiral fermions ($x_{t,b}$). Note that the W -matrix leads to an effective splitting of bottom and tau Yukawas of the type

$$y_\tau = y_b |c_\chi - x_b e^{i\varphi_b} s_\chi|. \quad (17)$$

On general grounds, additional sub-leading $SU(4)$ -breaking corrections are expected from integrating-out heavier fields.

- The 2×1 vectors $\vec{n}_{u,d}$ and \vec{n}_e are spurions parameterizing the $SU(4)$ breaking in the Yukawa sector or, equivalently, the breaking of the $U(2)_q$ and $U(2)_\ell$ flavor symmetries preventing heavy \leftrightarrow light mixing amongst chiral fermions [19, 21]. Given the field content in Table I, these terms are forbidden at the renormalizable level. In the limit $\vec{n}_{u,d} \rightarrow 0$, the only source of $U(2)_q$ breaking (besides the smaller light family Yukawa couplings) comes from s_q . As we shall show (see also [35]), this case is severely constrained by $\Delta F = 2$ observables. This is why we consider a small but non-negligible \vec{n}_u of the form $\vec{n}_u = (-y_t \epsilon_U e^{i\varphi_U} \ 0)^\top$, with $\epsilon_U = O(|V_{ub}|)$. As we show in Appendix B, this structure can be easily generated by integrating out a heavy vector-like quark $U_{L,R}$, charged under $SU(3)_L$, that mixes with t_R after 4321 symmetry breaking. Since the mixing required to generate V_{ub} is small, these new states could naturally be part of deeper UV dynamics in the 10-100 TeV range as occurs in [28].

Since $U(3)_{q,\ell}$ rotations leave the VL mass invariant, the 3×3 upper sub-block of the Yukawas can be diagonalized by bi-unitary rotations of the form $L_u \mathbf{Y}_u R_u^\dagger = \hat{\mathbf{Y}}_u$, $L_d \mathbf{Y}_d R_d^\dagger = \hat{\mathbf{Y}}_d$, and $L_e \mathbf{Y}_e R_e^\dagger = \hat{\mathbf{Y}}_e$, where $\hat{\mathbf{Y}}_{u,d,e}$ are diagonal in the 3×3 sub-block above the solid line and unchanged below it. In terms of these rotation matrices, the quark Yukawas can be written as

$$-\mathcal{L} \supset \bar{\Psi}_q L_u^\dagger \hat{\mathbf{Y}}_u R_u \tilde{H} \Psi_u + \bar{\Psi}_q L_d^\dagger \hat{\mathbf{Y}}_d R_d H \Psi_d + \text{h.c.} \quad (18)$$

The lepton Yukawas follow similarly, where acceptable neutrino masses can be achieved via the inverse-seesaw mechanism [24]. With these definitions, the CKM matrix is defined as $V_{\text{CKM}} = L_u L_d^\dagger$. Explicit formulas for these rotation matrices, in terms of the parameters appearing in (14)–(16) (including those *hidden* in $\hat{Y}_{u,d,e}$ and $\hat{U}_{u,d,e}$) are given in Appendix A.

III. $\Delta F = 2$ OBSERVABLES

Before EW symmetry breaking, we define the effective operator

$$\mathcal{O}_{qq}^{ijkl} = (\bar{q}_L^i \gamma_\mu q_L^j)(\bar{q}_L^k \gamma_\mu q_L^l), \quad (19)$$

such that the part of the effective Lagrangian relevant for $\Delta F = 2$ transitions can be written as

$$\mathcal{L}_{\text{eff}} \supset -\frac{4G_U}{\sqrt{2}} \sum_{ijkl} C_{qq}^{ijkl} \mathcal{O}_{qq}^{ijkl} + \text{h.c.}, \quad (20)$$

where the sum is over $i, j, k, l = 1, 2, 3$, and $G_U = G_F C_U$, where we have defined

$$C_U = \frac{g_4^2 v^2}{4m_{U_1}^2}, \quad (21)$$

that controls the strength of the purely third-generation contact interactions generated by integrating out the U_1 LQ. The flavor-conserving Wilson coefficients C_{qq}^{iiii} and C_{qq}^{jjjj} receive contributions from tree-level G' and Z' exchange, as well as from the U_1 vector LQ at one loop if $i \vee j = 2 \vee 3$, while the flavor-violating terms with $i \neq j \vee k \neq l$ receive only loop contributions. At the matching scale, the contribution to the various Wilson coefficients C_{qq}^{ijkl} are reported in Table II of Appendix D.

A. $B_{s(d)} - \bar{B}_{s(d)}$ mixing

We start by briefly summarizing the case of $B_{s(d)} - \bar{B}_{s(d)}$, which has been extensively discussed in the previous literature (see e.g. [35–37]). In this case we are interested in matching to the following effective operators after EW symmetry breaking

$$\mathcal{L} \supset -C_{B_s}^1 (\bar{s}_L \gamma_\mu b_L)^2 - C_{B_d}^1 (\bar{d}_L \gamma_\mu b_L)^2. \quad (22)$$

Performing the left-handed diagonalization of Yukawa matrices, the complete expressions for $C_{B_{s(d)}}^1$ are

$$C_{B_s}^1 = \frac{4G_U}{\sqrt{2}} \sum_{ijkl} L_d^{si} L_d^{sk} C_{qq}^{ijkl} (L_d^{bj})^* (L_d^{bl})^*, \quad (23)$$

$$C_{B_d}^1 = \frac{4G_U}{\sqrt{2}} \sum_{ijkl} L_d^{di} L_d^{dk} C_{qq}^{ijkl} (L_d^{bj})^* (L_d^{bl})^*. \quad (24)$$

Expanding the L_d matrices to the first non-trivial order, and taking into account the relevant Wilson coefficients reported in Table II, both at tree- and one-loop- level, leads to

$$C_{B_s}^1 = \frac{4G_U}{\sqrt{2}} e^{2i\phi_b} \left(\rho_q^{\text{NLO}} s_b^2 + e^{-2i\phi_b} \frac{\alpha_4}{8\pi} s_q^2 B_{qq}^{1221} \right), \quad (25)$$

$$C_{B_d}^1 = s_d^2 e^{2i\phi_d} C_{B_s}^1. \quad (26)$$

In these expressions, we defined

$$\rho_q^{\text{NLO}} = \left(\frac{1}{3x_{G'}} + \frac{1}{24x_{Z'}} + \frac{\alpha_4}{16\pi} \right), \quad (27)$$

where $x_V = m_V^2/m_{U_1}^2$ and $\alpha_4 = g_4^2/(4\pi)$: this coefficient encodes the effect of flavor-conserving Wilson coefficients generated by the tree-level G' and Z' exchange, and corresponding dominant next-to-leading order (NLO) corrections (in the $SU(4)_V$ custodial limit). The second term in $C_{B_s}^1$ is due to the flavor-violating Wilson coefficient C_{qq}^{2323} which is generated at one-loop.

The implications of these expressions, taking into account the experimental bounds on $B_{s(d)} - \bar{B}_{s(d)}$ mixing and the preferred range of G_U and s_q implied by the B anomalies, can be summarized as follows [37]:

- $s_b \lesssim 0.2|V_{ts}|$ is required to ensure a sufficient suppression of the flavor-conserving part of the amplitude, which is dominantly induced by tree-level G' exchange.
- Light vector-like leptons $m_L \lesssim 1.5$ TeV are required to ensure sufficient suppression of the B_{qq}^{1221} flavor-violating loop contribution, coming dominantly from box diagrams involving the U_1 LQ.

The mild down-alignment required in the 23 quark sector discussed in the first point is the main motivation behind the power-counting adopted in (A7) to organize the parameters appearing in the Yukawa couplings.

B. $K - \bar{K}$ and $D - \bar{D}$ mixing

After EW symmetry breaking, the effective operators describing neutral meson mixing involving only light quarks are

$$\mathcal{L} \supset -C_K^1 (\bar{d}_L \gamma_\mu s_L)^2 - C_D^1 (\bar{u}_L \gamma_\mu c_L)^2. \quad (28)$$

Again performing the left-handed diagonalization of Yukawa matrices, the expressions for $C_{K,D}^1$ read

$$C_K^1 = \frac{4G_U}{\sqrt{2}} \sum_{ijkl} L_d^{di} L_d^{dk} C_{qq}^{ijkl} (L_d^{sj})^* (L_d^{sl})^*, \quad (29)$$

$$C_D^1 = \frac{4G_U}{\sqrt{2}} \sum_{ijkl} L_u^{ui} L_u^{uk} C_{qq}^{ijkl} (L_u^{cj})^* (L_u^{cl})^*. \quad (30)$$

In both cases the sum is dominated by the flavor conserving Wilson coefficients, which receive tree-level contributions from G' and Z' exchange. Given the power-counting in (A7) (i.e. working in the limit $s_b \rightarrow 0$) the leading contributions are

$$C_K^1 = \frac{4G_U}{\sqrt{2}} \rho_q^{\text{NLO}} s_q^4 (V_{us} + c_d s_u e^{i\phi_u})^2 c_d^2 / c_u^2, \quad (31)$$

$$C_D^1 = \frac{4G_U}{\sqrt{2}} \rho_q^{\text{NLO}} (c_u s_u s_q^2 e^{i\phi_u} - e^{-i\delta} |V_{ub}| |V_{cb}|)^2, \quad (32)$$

where in C_K^1 we have used the CKM relation $V_{us} = e^{i\phi_d} c_u s_d - e^{i\phi_u} c_d s_u$ from Eq. (A20). According to data on the anomalies, C_U lies in the range $0.004 \leq C_U \leq 0.03$. In the $SU(4)_V$ custodial limit (where the heavy-vector spectrum is approximately degenerate), we have $\rho_{[q]}^{\text{NLO}} \approx 0.4$. Due to the strong scaling of $C_{K,D}^1$ with s_q , we focus on two benchmark points (BPs) near the upper end of the C_U range, in order to maximize the contribution to $\delta R_{D^{(*)}}$ (defined in (C1) and (C2)),

$$\text{BP1: } C_U = 0.015, \quad (33)$$

$$\text{BP2: } C_U = 0.030. \quad (34)$$

In both cases we assume $x_{G'} = x_{Z'} = 1$ unless otherwise specified.

The strongest constraints are those on the imaginary parts of $C_{K,D}^1$. According to [38, 39] the 95% confidence allowed range is

$$\text{Im}(C_K^1) = [-1.2, 2.4] \times 10^{-9} \text{ TeV}^{-2}, \quad (35)$$

$$\text{Im}(C_D^1) = [-9.4, 8.9] \times 10^{-9} \text{ TeV}^{-2}. \quad (36)$$

Comparing the expressions for $C_{K,D}^1$ to the bounds in (35)–(36), it is clear that a precise flavor-alignment pattern is needed to satisfy the $\Delta F = 2$ bounds if $|s_q| \gtrsim |V_{cb}|$, as required by the best fit of the charged-current anomalies. Starting with $D-\bar{D}$ mixing, we see from Fig. 1 that the simplest solution to pass the bound on $\text{Im}(C_D^1)$ is a mild *up-alignment*: the angle s_u , controlling the 12 up-quark rotation hence naturally expected to be of $O(|V_{us}|)$, cannot exceed 10% of $|V_{us}|$. This result is largely independent from the value of ϕ_u .

Assuming this mild up-alignment, we now move to the analysis of $K-\bar{K}$ mixing. Neglecting terms $O(s_u^2)$, the following simplified expression holds

$$\text{Im}(C_K^1) \approx \frac{8G_U}{\sqrt{2}} \rho_q^{\text{NLO}} V_{ud}^3 V_{us} s_q^4 s_u \sin \phi_u, \quad (37)$$

and we see that the size of CP violation in kaon mixing is controlled by s_q and the product $s_u \sin \phi_u$. As shown in Fig. 2, the latter product is severely constrained for $|s_q| \gtrsim |V_{cb}|$. However, it is worth noticing that $s_u \sin \phi_u = 0$ is achieved either assuming $\phi_u = 0$ (hence CP conservation) or in the limit of exact up-alignment (i.e. for $s_u = 0$).

In principle, an alternative solution also exists, as shown in the upper half of Fig. 1. However, for this solution to pass both $K-\bar{K}$ and $D-\bar{D}$ mixing bounds, a strong but not exact down-alignment is needed, $|s_d| \approx$

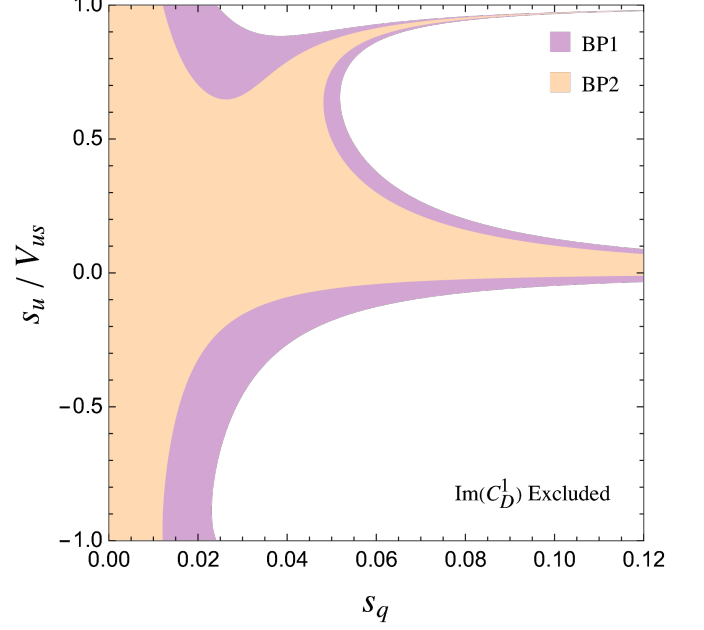


FIG. 1. Constraints from CP violation in $D-\bar{D}$ mixing on the light quark mixing angle s_u as a function of s_q , assuming a generic $\mathcal{O}(1)$ value for the phase Δ_{ud} (see Appendix A). The areas outside the colored regions (corresponding to the two benchmark points) are excluded by the bounds on $\text{Im}C_D^1$ at the 95% confidence level.

$\text{Im}(V_{ub}^* V_{cb})/s_q^2$, and the phase difference Δ_{ud} (defined in Appendix A) need to be set to $\Delta_{ud} \sim \text{sgn}(s_d \cos \phi_u) \pi/2$. We find these conditions more difficult to justify from a UV model point of view, being far from a clear symmetric limit. For this reason, in the following we focus on the up-aligned solution.

In summary, to pass the bounds on $\text{Im}(C_{K,D}^1)$ we require: i) $|s_u| \ll |V_{us}|$ and (depending on the degree of up-alignment) ii) $\phi_u \approx 0$, corresponding to the assumptions of i) up-alignment for the 2×2 light-quark Yukawa couplings and ii) approximate CP conservation.

Turning our attention now to the real parts of the $\Delta F = 2$ amplitudes, in the limit $s_u \approx 0$ only $K-\bar{K}$ mixing receives a sizable contribution

$$\text{Re}(C_K^1) \approx \frac{4G_U}{\sqrt{2}} \rho_q^{\text{NLO}} V_{ud}^2 V_{us}^2 s_q^4, \quad (38)$$

which is dominantly controlled by s_q . This induces a non-standard contribution to the $K-\bar{K}$ mass difference, that we can write as

$$\delta m_K = \frac{\Delta m_K^{\text{NP}}}{\Delta m_K^{\text{exp}}} = \frac{2}{3} \frac{m_K}{\Delta m_K^{\text{exp}}} F_K^2 P_1^{\text{VLL}} \text{Re}(C_K^1), \quad (39)$$

where $m_K = 497.6 \text{ MeV}$, $\Delta m_K^{\text{exp}} = 3.484 \times 10^{-12} \text{ MeV}$, $F_K = 160 \text{ MeV}$, and $P_1^{\text{VLL}}(\mu_K) = 0.48$ encodes the bag parameter and QCD corrections [40]. Numerically, we find

$$\delta m_K \approx 1.086 \times \left(\frac{C_U}{0.015} \right) \left(\frac{s_q}{0.1} \right)^4. \quad (40)$$

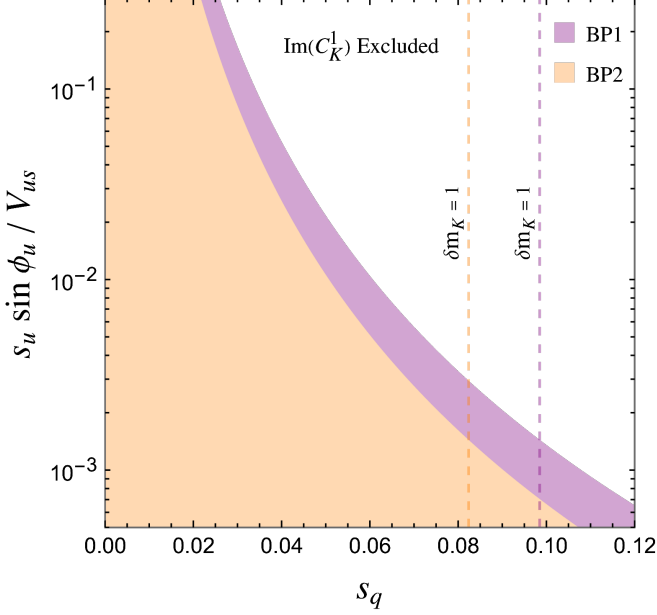


FIG. 2. Constraints from CP violation in $K\text{--}\bar{K}$ mixing on the combination $s_u \sin \phi_u$ as a function of s_q . The area outside the colored regions (corresponding to our two benchmark points) is excluded by the bounds on $\text{Im}(C_K^1)$ at the 95% confidence level. The vertical lines denote indicative upper bounds on s_q set by $\text{Re}(C_K^1)$.

In view of the long-distance contributions to Δm_K , we can translate this result into a bound on the size of $|s_q| \lesssim 0.1$ for the preferred range of C_U .

C. Summary on the mixing structure

What emerges from the previous discussion can be summarized as follows:

- *Structure of the Yukawa couplings.* The mixing of light families in the CKM (i.e. the Cabibbo angle) is induced mainly by the down Yukawa coupling \mathbf{Y}_d . On the other hand, heavy \leftrightarrow light mixing and the CKM phase are generated mainly by \mathbf{Y}_u .
- *Light \leftrightarrow vector-like mixing.* The parameter s_q , which controls the largest breaking of $U(2)_q$ and plays a key role in all the LFU ratios, cannot exceed 0.1 in magnitude.

IV. $K \rightarrow \pi \nu \bar{\nu}$

We now proceed to analyze the implications of the mixing structure determined in Section III on $K \rightarrow \pi \nu \bar{\nu}$ decays. In the EW-symmetric phase, we define the semi-leptonic operator

$$\mathcal{O}_{\ell q}^{\alpha\beta ij} = (\bar{\ell}_L^\alpha \gamma_\mu \ell_L^\beta)(\bar{q}_L^i \gamma^\mu q_L^j). \quad (41)$$

Our setup is such that only $s \rightarrow d \nu \nu$ transitions involving third-generation neutrinos receive large NP corrections.² Therefore, the relevant part of the effective Lagrangian reads

$$\mathcal{L}_{\text{eff}} \supset -\frac{4G_U}{\sqrt{2}} \sum_{ij} C_{\ell q}^{33ij} \mathcal{O}_{\ell q}^{33ij} + \text{h.c.}, \quad (42)$$

where the sum runs over $i, j = 1, 2, 3$. The relevant contributions to this process come from the tree-level Z' exchange for the flavor-conserving Wilson coefficients $C_{\ell q}^{33ii}$ as well as from one-loop diagrams involving the U_1 leptoquark for flavor-conserving and flavor-violating Wilson coefficients $C_{\ell q}^{33ij}$, with $i \vee j = 2 \vee 3$. These contributions are reported at the bottom of Table II in Appendix D.

Similarly to the case of $b \rightarrow s \nu \nu$ transitions (see e.g. [19, 26]) there is no tree-level contribution mediated by the U_1 LQ to $s \rightarrow d \nu \nu$ amplitudes. This is because the tree-level U_1 exchange generates both $SU(2)_L$ -singlet semi-leptonic operators as in (42) as well as their $SU(2)_L$ -triplet counterparts, $(\bar{\ell}_L^3 \gamma_\mu \tau_a \ell_L^3)(\bar{q}_L^i \gamma^\mu \tau^a q_L^j)$, with the same Wilson coefficient, resulting in a cancellation. This structure is simply a consequence of the U_1 gauge quantum numbers, which forbid its coupling to down-type quarks and neutrinos.

After EW symmetry is broken, we project the contributions of (42) onto the coefficients of the operators $(\bar{s}_L \gamma_\mu d_L)(\bar{\nu}_\ell \gamma^\mu \nu_\ell)$, that we normalize as in the SM

$$\mathcal{L}_{\text{eff}} = -\frac{4G_F}{\sqrt{2}} \frac{\alpha_W}{2\pi} V_{ts}^* V_{td} \sum_{\ell=e,\mu,\tau} C_\ell (\bar{s}_L \gamma_\mu d_L)(\bar{\nu}_\ell \gamma^\mu \nu_\ell), \quad (43)$$

where $\alpha_W = g_2^2/(4\pi)$ and V_{ij} are CKM matrix elements. Using the results in [11], we decompose $\mathcal{B}(K^+ \rightarrow \pi^+ \nu \nu)$ and $\mathcal{B}(K_L \rightarrow \pi^0 \nu \nu)$ in terms of the C_ℓ as

$$\mathcal{B}(K^+ \rightarrow \pi^+ \nu \nu) = \mathcal{B}_+ \sum_{\ell=e,\mu,\tau} \left\{ [\text{Im}(V_{ts}^* V_{td} C_\ell)]^2 + [|V_{us}|^5 |V_{cs}| P_c - \text{Re}(V_{ts}^* V_{td} C_\ell)]^2 \right\}, \quad (44)$$

$$\mathcal{B}(K_L \rightarrow \pi^0 \nu \nu) = \mathcal{B}_L \sum_{\ell=e,\mu,\tau} [\text{Im}(V_{ts}^* V_{td} C_\ell)]^2, \quad (45)$$

where $B_+ = 2.62 \times 10^{-6}/|V_{us}|^2$ and $B_L = 4.16 \times 10^{-6}/|V_{us}|^2$. Within the SM,

$$C_{e,\mu,\tau}^{\text{SM}} \equiv X_t, \quad (46)$$

with $X_t = 1.48 \pm 0.01$ [41], while the parameter encoding the long-distance contribution due to charm and light-quark loops (averaged over the different lepton species) is $P_c = 0.404 \pm 0.024$.³

² The leading correction is suppressed relative to the third-generation contribution by s_ℓ^2 .

³ In principle, P_c is different for the different lepton species; however, we have explicitly checked that this effect is negligible compared to the model uncertainties affecting ΔC_τ .

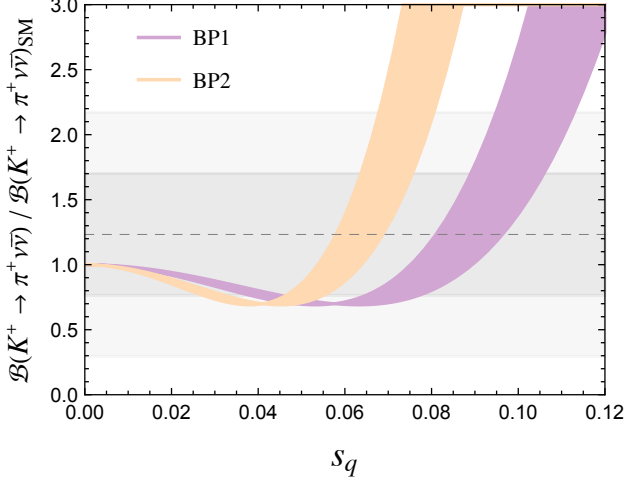


FIG. 3. Prediction for $\mathcal{B}(K^+ \rightarrow \pi^+ \nu \bar{\nu})$, normalized to the SM, as a function of s_q for the two benchmark points we have considered (setting $\theta_\chi = \pi/4$, $m_L = 1$ TeV, $m_Q = 1.5$ TeV). The colored bands are generated by varying $g_A \in [2, 3]$ and $x_{Z'} \in [0.8, 1]$. The gray regions show the current experimental determination of $\mathcal{B}(K^+ \rightarrow \pi^+ \nu \bar{\nu})$ at $\pm 1\sigma$ and $\pm 2\sigma$.

Within our framework, (44)–(45) remain valid and the only modification compared to the SM case is the value of C_τ , that we decompose as

$$C_\tau \approx C_\tau^{\text{SM}} [1 + \rho \Delta C_\tau]. \quad (47)$$

Running (42) down to the EW scale, and working in the basis where the down Yukawa coupling is diagonal we get

$$\Delta C_\tau = \frac{1}{V_{ts}^* V_{td}} \sum_{ij} L_d^{si} \left[\mathcal{C}_{\ell q}^{33ij} + \beta_L^{i3} (\beta_L^{j3})^* \mathcal{C}_U^{\text{RGE}} \right] (L_d^{dj})^*,$$

$$\rho = \frac{2\pi}{\alpha_W X_t} C_U = 1.26 \times \left(\frac{C_U}{0.01} \right). \quad (48)$$

The contributions of the flavor-violating Wilson coefficients to (48) are suppressed by the 23 and 13 down rotations, which are required to be small in order to evade the bounds on $B_{s(d)}$ mixing. As a consequence, the sum over $\mathcal{C}_{\ell q}^{33ij}$ is dominated by the flavor conserving Wilson coefficients, which receive a Cabbibo-sized rotation

$$\sum_{ij} L_d^{si} \mathcal{C}_{\ell q}^{33ij} (L_d^{dj})^* \approx (\mathcal{C}_{\ell q}^{3311} - \mathcal{C}_{\ell q}^{3322}) c_d s_d e^{-i\phi_d}. \quad (49)$$

The leading correction to this result that, as expected, vanishes in the $U(2)_q$ symmetric limit, is $\mathcal{O}(s_b/s_q)$. Similarly, the leading contribution to the $\mathcal{C}_U^{\text{RGE}}$ term encoding the RG evolution of tree-level leptoquark mediated operators is given by the $i = j = 2$ term

$$L_d^{s2} \beta_L^{23} (\beta_L^{23} L_d^{d2})^* = -c_d s_d e^{-i\phi_d} |W_{21}|^2 s_q^2. \quad (50)$$

Using DsixTools [42] and setting $m_{U_1} = 4$ TeV, we find

$$\mathcal{C}_U^{\text{RGE}} \approx -0.058. \quad (51)$$

Using the CKM relation $V_{us} = e^{i\phi_d} c_u s_d - e^{i\phi_u} c_d s_u$ from Eq. (A20), we obtain a final expression for ΔC_τ that is dominantly controlled by s_q in the up-aligned limit:

$$\Delta C_\tau \approx s_q^2 \frac{V_{us}^* V_{ud}}{V_{ts}^* V_{td}} \left[\frac{1}{4x_{Z'}} + \frac{\alpha_4}{4\pi} B_{q\ell}^{2211} - |W_{21}|^2 \mathcal{C}_U^{\text{RGE}} \right]. \quad (52)$$

Importantly, the phase of ΔC_τ is fully specified, leading to the following conclusions:

- $\text{Im}(V_{ts}^* V_{td} \Delta C_\tau) \approx 0 \rightarrow$ negligible correction compared to the SM in $\mathcal{B}(K_L \rightarrow \pi^0 \nu \bar{\nu})$;
- $\text{Re}(V_{ts}^* V_{td} \Delta C_\tau) > 0 \rightarrow$ negative interference between NP and SM amplitudes in $\mathcal{B}(K^+ \rightarrow \pi^+ \nu \bar{\nu})$.

The prediction of $\mathcal{B}(K^+ \rightarrow \pi^+ \nu \bar{\nu})$ thus obtained, as a function of s_q , for the two benchmarks defined in Section III is shown in Fig. 3. As can be seen, $\mathcal{B}(K^+ \rightarrow \pi^+ \nu \bar{\nu})$ exhibits a strong and well-defined dependence on s_q , which will be extremely valuable in determining this parameter from data in the near future. Interestingly enough, the current experimental measurement of $\mathcal{B}(K^+ \rightarrow \pi^+ \nu \bar{\nu})$ [12], even if affected by a sizable error, already provides a non-trivial constraint on the model. In fact, for benchmark point 2, the bound on $|s_q|$ we determine from $\mathcal{B}(K^+ \rightarrow \pi^+ \nu \bar{\nu})$ is more stringent than the one derived from $\Delta F = 2$ observables.

In Fig. 4, we show the correlation between $\mathcal{B}(K^+ \rightarrow \pi^+ \nu \bar{\nu})$ and the two LFU ratios in charged-current B decays, which also exhibit a strong (but different) dependence on s_q . In particular, what we show in Fig. 4 are the relative corrections

$$\delta R_{D^{(*)}} = \frac{R_{D^{(*)}}}{R_{D^{(*)}}^{\text{SM}}} - 1, \quad (53)$$

that we compute using the NLO expressions [26] reported in Appendix C. Contrary to all the observables discussed so far, R_D and R_{D^*} are sensitive to the coupling of the leptoquark field to third-generation RH chiral fermions (parameterized in terms of the effective coupling $\beta_R^{b\tau}$). In the minimal version of the model, $|\beta_R^{b\tau}| = 1$; however, in less minimal frameworks different values could be obtained with additional sets of VL fermions.⁴ For illustrative purposes and also to connect with previous studies [37], in the following we consider two choices for $\beta_R^{b\tau}$ in relation to the two benchmarks considered so far:

$$\text{BP1 } [C_U = 0.015]: \quad \text{Re}(\beta_R^{b\tau}) = -0.3, \quad (54)$$

$$\text{BP2 } [C_U = 0.030]: \quad \text{Re}(\beta_R^{b\tau}) = 0. \quad (55)$$

A non-vanishing $\beta_R^{b\tau}$ mainly impacts R_D , which is particularly sensitive to scalar-current contributions. This

⁴ One example is the introduction of $SU(3)_L$ -charged VL partners of the light family right-handed fields, as in Appendix B.

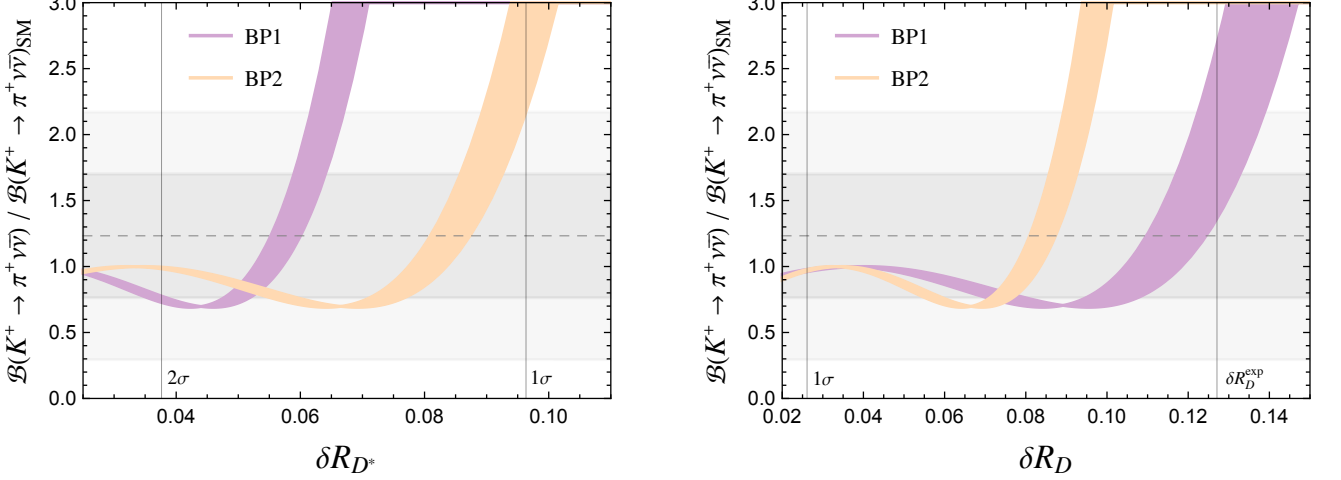


FIG. 4. Prediction for $\mathcal{B}(K^+ \rightarrow \pi^+ \nu \bar{\nu})$, normalized to the SM, vs. the relative modifications of the LFU ratios R_{D^*} (left) and R_D (right), also normalized to the SM. The notation and parameters are the same as in Fig. 3, and the colored bands are again generated by varying $g_4 \in [2, 3]$ and $x_{Z'} \in [0.8, 1]$. The vertical lines indicate the current experimental determination of the LFU ratios at different levels of significance.

is illustrated by the comparison of left and right plots in Fig. 4. We finally stress that the value of C_U , which is the main parameter distinguishing the different curves in Fig. 4, could in principle be determined from high-energy data, in particular from $\sigma(pp \rightarrow \tau^+ \tau^-)$ [37]. In the future, the combination of precision measurements of R_D , R_{D^*} , and $\mathcal{B}(K^+ \rightarrow \pi^+ \nu \bar{\nu})$, combined with high-energy data on $\sigma(pp \rightarrow \tau^+ \tau^-)$, should result in decisive tests of this framework.

V. CONCLUSIONS

The non-universal 4321 gauge model featuring third-family quark-lepton unification represents a very attractive extension of the SM. On the theoretical side, it can arise as the low-energy limit of ambitious UV models addressing both the origin of quark and lepton mass hierarchies, as well as the electroweak hierarchy problem [23, 28, 34]. On the phenomenological side, it predicts the existence of a TeV-scale vector leptoquark that could account for the hints of LFU violation observed in semi-leptonic B -meson decays.

As we have shown, the minimal version of the model is quite constrained by low-energy observables, resulting in a predictive framework not only for the leading $3 \rightarrow 2$ flavor-changing transitions, but also for processes involving light quarks only. In this context, precise measurements of $K \rightarrow \pi \nu \bar{\nu}$ decay rates can play a key role in further testing this setup.

Confirming previous findings obtained in different SM extensions [13–16], we find sizable deviations from the SM in $\mathcal{B}(K^+ \rightarrow \pi^+ \nu \bar{\nu})$, within the parameter space motivated by the B -meson anomalies. Most importantly, as illustrated in Fig. 4, a well-defined pattern of correla-

tions between $\mathcal{B}(K^+ \rightarrow \pi^+ \nu \bar{\nu})$, R_D , and R_{D^*} , emerges. Testing these correlations, with future precision measurements of these low-energy observables, would provide an extremely valuable test of this motivated framework.

ACKNOWLEDGEMENTS

This project has received funding from the European Research Council (ERC) under the European Union’s Horizon 2020 research and innovation programme under grant agreement 833280 (FLAY), and by the Swiss National Science Foundation (SNF) under contract 200020_204428.

Appendix A: Yukawa Diagonalization and the CKM Matrix

The Yukawas can be brought to diagonal form in the 3×3 sub-block by rotations of the form $L_u \mathbf{Y}_u R_u^\dagger = \hat{\mathbf{Y}}_u$, $L_d \mathbf{Y}_d R_d^\dagger = \hat{\mathbf{Y}}_d$, and $L_e \mathbf{Y}_e R_e^\dagger = \hat{\mathbf{Y}}_e$. In terms of these rotation matrices, the Lagrangian takes the form

$$-\mathcal{L} \supset \bar{\Psi}_q L_u^\dagger \hat{\mathbf{Y}}_u R_u \tilde{H} \Psi_u + \bar{\Psi}_q L_d^\dagger \hat{\mathbf{Y}}_d R_d H \Psi_d + \bar{\Psi}_\ell L_e^\dagger \hat{\mathbf{Y}}_e R_e H \Psi_e + \text{h.c.} \quad (\text{A1})$$

These rotation matrices can be decomposed as the product of rotations in the $13 \times 23 \times 12$ sectors. For example, in the up sector we have

$$L_u = P_u L_u^{12} L_u^{23} L_u^{13}, \quad (\text{A2})$$

with

$$\begin{aligned}
L_u^{12} &= \begin{pmatrix} c_u & -e^{i\varphi_u} s_u & 0 & 0 \\ e^{-i\varphi_u} s_u & c_u & 0 & 0 \\ 0 & 0 & 1 & 0 \\ 0 & 0 & 0 & 1 \end{pmatrix}, \\
L_u^{13} &= \begin{pmatrix} c_{ut} & 0 & -e^{i\varphi_{ut}} s_{ut} & 0 \\ 0 & 1 & 0 & 0 \\ e^{-i\varphi_{ut}} s_{ut} & 0 & c_{ut} & 0 \\ 0 & 0 & 0 & 1 \end{pmatrix}, \\
L_u^{23} &= \begin{pmatrix} 1 & 0 & 0 & 0 \\ 0 & c_t & -e^{i\varphi_t} s_t & 0 \\ 0 & e^{-i\varphi_t} s_t & c_t & 0 \\ 0 & 0 & 0 & 1 \end{pmatrix},
\end{aligned} \tag{A3}$$

and $P_{u,d}$ are arbitrary phase diagonal matrices that we will fix later to match the standard CKM phase convention. The matching of the Lagrangian parameters in (14) onto the rotation matrix angles in L_u^{23} and L_u^{13} is

$$s_t = -x_t s_q, \quad e^{i\varphi_{ut}} s_{ut} = -e^{i\varphi_U} \epsilon_U, \tag{A4}$$

while L_u^{12} is in direct correspondence with the 2×2 matrix U_u .

There are also chirally suppressed RH rotations

$$\begin{aligned}
R_u^{23} &= \begin{pmatrix} 1 & 0 & 0 \\ 0 & 1 & -\frac{m_c}{m_t} e^{i\varphi_t} s_t \\ 0 & \frac{m_c}{m_t} e^{-i\varphi_t} s_t & 1 \end{pmatrix}, \\
R_u^{13} &= \begin{pmatrix} 1 & 0 & -\frac{m_u}{m_t} e^{i\varphi_{ut}} s_{ut} \\ 0 & 1 & 0 \\ \frac{m_u}{m_t} e^{-i\varphi_{ut}} s_{ut} & 0 & 1 \end{pmatrix},
\end{aligned} \tag{A5}$$

and $R_u = P_u R_u^{23} R_u^{13}$. The down quark and charged lepton rotations follow the same pattern, and can easily be written in terms of s_d, s_b, s_{db} and $s_e, s_\tau, s_{e\tau}$ with their corresponding phases.

1. CKM Matrix

To compute the CKM matrix,

$$V_{\text{CKM}} = L_u L_d^\dagger, \tag{A6}$$

we will work with the rotation matrices defined in the previous section and keep the angles arbitrary. The CKM computed in this way will be valid for any version of the model, since all that changes will be the matching of the model parameters onto the angles. We will compute the CKM matrix to $\mathcal{O}(\lambda^3)$ assuming the following power counting for the rotation matrix angles

$$\theta_{u,d} \sim \lambda, \quad \theta_t \sim \lambda^2, \quad \theta_b \sim \lambda^3, \quad \theta_{ut} \sim \lambda^3, \quad \theta_{db} \sim \lambda^4. \tag{A7}$$

It is convenient to define the following phases

$$\Delta_{ud} = \varphi_u - \varphi_d, \tag{A8}$$

$$\Delta_{tb} = \varphi_t - \varphi_b, \tag{A9}$$

$$\Delta_{ut} = \varphi_{ut} - \varphi_u - \varphi_t, \tag{A10}$$

$$\phi_1 = \arg(c_u c_d + e^{-i\Delta_{ud}} s_u s_d), \tag{A11}$$

$$\phi_u = \arg(e^{i\Delta_{ud}} c_u s_d - s_u c_d), \tag{A12}$$

$$\phi_t = \arg(-s_t + e^{i\Delta_{tb}} s_b), \tag{A13}$$

$$\phi_{ut} = \arg(s_u s_t - e^{i\Delta_{ut}} s_{ut}), \tag{A14}$$

$$\phi_d = \phi_u - \Delta_{ud}, \tag{A15}$$

$$\phi_b = \phi_t - \Delta_{tb}. \tag{A16}$$

We see that according to our power counting, if Δ_{ud} , Δ_{tb} and Δ_{ut} are order one, then we have $\phi_1 \sim \mathcal{O}(\lambda^2)$, $\sin \phi_t \sim \mathcal{O}(\lambda)$, and $\phi_{ut}, \phi_u, \phi_d, \phi_b \sim \mathcal{O}(1)$.

Choosing the arbitrary phase matrices

$$P_u = \text{diag}\{e^{i(\phi_u - \varphi_u + \phi_t - \varphi_t + \phi_1)}, e^{i(\phi_t - \varphi_t)}, 1, 1\}, \tag{A17}$$

$$P_d = \text{diag}\{e^{i(\phi_u - \varphi_u + \phi_t - \varphi_t)}, e^{i(\phi_t - \varphi_t + \phi_1)}, 1, 1\}, \tag{A18}$$

we find that the CKM takes the following form

$$V_{\text{CKM}} = \left(\begin{array}{ccc|c} V_{ud} & V_{us} & V_{ub} & 0 \\ V_{cd} & V_{cs} & V_{cb} & 0 \\ V_{td} & V_{ts} & V_{tb} & 0 \\ 0 & 0 & 0 & 1 \end{array} \right), \tag{A19}$$

where, at $\mathcal{O}(\lambda^3)$, we have

$$\begin{aligned}
V_{ud} &= e^{i\phi_1} (c_u c_d + e^{i\Delta_{ud}} s_u s_d) \\
V_{us} &= e^{i\phi_u} (e^{-i\Delta_{ud}} c_u s_d - s_u c_d) \\
V_{ub} &= e^{i(\phi_u + \phi_t + \phi_1)} (s_u s_t - e^{i\Delta_{ut}} s_{ut}) \\
V_{cd} &= -V_{us}^* \\
V_{cs} &= V_{ud}^* \\
V_{cb} &= e^{i\phi_t} (-s_t + e^{-i\Delta_{tb}} s_b) \\
V_{td} &= e^{-i(\phi_u + \phi_t)} (-e^{i\Delta_{ud}} s_d s_t + e^{-i\Delta_{ut}} s_{ut}) \\
V_{ts} &= -e^{-i\phi_1} V_{cb}^* \\
V_{tb} &= 1.
\end{aligned} \tag{A20}$$

We have chosen the phases in (A18) such that V_{ud}, V_{us} , and V_{cb} are real. At this order in λ , we have $V_{td} \approx V_{us}^* V_{cb}^* - V_{ub}^*$. The CKM phase, $V_{ub} = |V_{ub}| e^{-i\delta}$, is then

$$\delta = -(\phi_{ut} + \phi_u + \phi_t + \phi_1). \tag{A21}$$

2. Quark Rotation Matrices

Neglecting the small ϕ_1 phase and working to $\mathcal{O}(\lambda^3)$, we find the quark rotation matrices to be

$$\begin{aligned}
L_d &= P_d L_d^{12} L_d^{23} L_d^{13} = \\
&\left(\begin{array}{ccc|c} c_d & -e^{i\phi_d} s_d & 0 & 0 \\ e^{-i\phi_d} s_d & c_d & -e^{i\phi_b} s_b & 0 \\ 0 & e^{-i\phi_b} s_b & 1 & 0 \\ 0 & 0 & 0 & 1 \end{array} \right) P_q,
\end{aligned} \tag{A22}$$

$$L_u = P_u L_u^{12} L_u^{23} L_u^{13} =$$

$$\left(\begin{array}{ccc|c} c_u & -e^{i\phi_u} s_u & |V_{ub}|e^{-i\delta} & 0 \\ e^{-i\phi_u} s_u & c_u & -e^{i\phi_t} s_t & 0 \\ \hline e^{-i(\phi_u+\phi_t)} s_u s_t - |V_{ub}|e^{i\delta} & e^{-i\phi_t} s_t & 1 & 0 \\ 0 & 0 & 0 & 1 \end{array} \right) P_q, \quad (\text{A23})$$

where

$$P_q = \text{diag}\{e^{i(\phi_u-\varphi_u+\phi_t-\varphi_t)}, e^{i(\phi_t-\varphi_t)}, 1, 1\}. \quad (\text{A24})$$

Appendix B: $SU(3)_l$ Vector-like Fermions

We extend the matter content given in Table I by a new vector-like quark with quantum numbers $U_{L,R} \sim (\mathbf{1}, \mathbf{3}, \mathbf{1}, 2/3)$ under \mathcal{G}_{4321} . The addition of this state extends the flavor symmetry as $U(2)_{u_R} \rightarrow U(3)_{u_R} \times U(1)_{U_L}$, where we have defined a vector $\mathcal{U}_R^\top = (u_R^1, u_R^2, U_R)$. The new terms one can write in the Lagrangian are

$$-\mathcal{L} \supset \bar{U}_L \hat{M}_U \mathcal{U}_R + \lambda_U \bar{U}_L \Omega_3 \psi_R^\dagger + \bar{q}_L \mathbf{y}_U \tilde{H} U_R + \text{h.c.}, \quad (\text{B1})$$

where without loss of generality we can use the $U(3)_{u_R}$ to put the 1×3 mass in the form $\hat{M}_U = (0 \ 0 \ m_U)$ with m_U real and the $U(1)_{U_L}$ to make the complex number λ_U real. In this basis, \mathbf{y}_U is an arbitrary 2×1 complex vector, where we define $\mathbf{y}_U^\top = (y_U^1 e^{i\varphi_U^1}, y_U^2 e^{i\varphi_U^2})$. In total, we removed 4 phases and 2 real parameters, which is consistent since the flavor symmetry was enlarged from $U(2)_{u_R} \rightarrow U(3)_{u_R} \times U(1)_{U_L}$, meaning we are allowed to remove $6+1-3=4$ phases and $3-1=2$ real parameters. Finally, it is clear that this part of the Lagrangian leaves a $U(2)_{u_R}$ subgroup unbroken, while the coupling \mathbf{y}_U is a new source of $U(2)_q$ symmetry breaking.

1. 4321 Broken Phase

After 4321 symmetry breaking, let us define $\Psi_u^\top = (u_R^1, u_R^2, u_R^3, U_R)$. We then have to diagonalize the mixing between u_R^3 and U_R

$$\bar{U}_L \begin{pmatrix} 0 & 0 & \frac{\lambda_U v_3}{\sqrt{2}} & m_U \end{pmatrix} \Psi_u = \bar{U}_L \begin{pmatrix} 0 & 0 & 0 & m_U^{\text{phys}} \end{pmatrix} W_u \Psi_u, \quad (\text{B2})$$

where

$$m_U^{\text{phys}} = \sqrt{m_U^2 + \frac{1}{2} \lambda_U^2 v_3^2}, \quad (\text{B3})$$

and W_u is an orthogonal rotation mixing u_R^3 and U_R

$$W_u = \begin{pmatrix} 1 & 0 & 0 & 0 \\ 0 & 1 & 0 & 0 \\ 0 & 0 & c_U & -s_U \\ 0 & 0 & s_U & c_U \end{pmatrix}, \quad (\text{B4})$$

where the mixing angle is defined as

$$\tan \theta_U = \frac{\lambda_U v_3}{\sqrt{2} m_U}. \quad (\text{B5})$$

2. Yukawas

After rotating to the fermion mass basis, the up Yukawa

$$-\mathcal{L} \supset \bar{\Psi}_q \mathbf{Y}_u \tilde{H} \Psi_u + \text{h.c.}, \quad (\text{B6})$$

can be written as a 4×4 matrix

$$\begin{aligned} \mathbf{Y}_u &= \mathbf{O}_q \left(\begin{array}{cc|c} U_u^\dagger \hat{Y}_u & 0 & \mathbf{y}_U \\ 0 & y_t & 0 \\ \hline 0 & y_t x_t e^{i\varphi_t} & 0 \end{array} \right) W_u^\dagger \\ &= \mathbf{O}_q \left(\begin{array}{ccc|c} y_u c_u & y_c e^{i\varphi_u} s_u & -y_U^1 e^{i\varphi_U^1} s_U & y_U^1 e^{i\varphi_U^1} c_U \\ -y_u e^{-i\varphi_u} s_u & y_c c_u & -y_U^2 e^{i\varphi_U^2} s_U & y_U^2 e^{i\varphi_U^2} c_U \\ \hline 0 & 0 & y_t c_U & y_t s_U \\ 0 & 0 & y_t x_t e^{i\varphi_t} c_U & y_t x_t e^{i\varphi_t} s_U \end{array} \right) \\ &= \left(\begin{array}{ccc|c} y_u c_u & y_c e^{i\varphi_u} s_u & -y_U^1 e^{i\varphi_U^1} s_U & y_U^1 e^{i\varphi_U^1} c_U \\ -y_u e^{-i\varphi_u} s_u c_q & y_c c_u c_q & -y_U^2 e^{i\varphi_U^2} s_U c_q - y_t x_t e^{i\varphi_t} c_U s_q & y_U^2 e^{i\varphi_U^2} c_U c_q - y_t x_t e^{i\varphi_t} s_U s_q \\ \hline 0 & 0 & y_t c_U & y_t s_U \\ -y_u e^{-i\varphi_u} s_u s_q & y_c c_u s_q & y_t x_t e^{i\varphi_t} c_U c_q - y_U^2 e^{i\varphi_U^2} s_U s_q & y_t x_t e^{i\varphi_t} s_U c_q + y_U^2 e^{i\varphi_U^2} c_U s_q \end{array} \right). \end{aligned} \quad (\text{B7})$$

In the limit of small θ_U (corresponding to integrating out the new vector-like state $U_{L,R}$), the 4×3 sub-block reads

$$\mathbf{Y}_u = \begin{pmatrix} y_u c_u & y_c e^{i\varphi_u} s_u & -y_U^1 e^{i\varphi_U^1} s_U \\ -y_u e^{-i\varphi_u} s_u c_q & y_c c_u c_q & -y_t x_t e^{i\varphi_t} s_q \\ 0 & 0 & y_t \\ -y_u e^{-i\varphi_u} s_u s_q & y_c c_u s_q & y_t x_t e^{i\varphi_t} c_q \end{pmatrix}, \quad (\text{B8})$$

which reproduces the structure we wanted in Section II A and we identify $y_t \epsilon_U e^{i\varphi_U} = y_U^1 e^{i\varphi_U^1} s_U$. We therefore generate V_{ub} with the right size for

$$y_U^1 \sin \theta_U \approx \frac{y_U^1 \lambda_U}{\sqrt{2}} \frac{v_3}{m_U} \approx |V_{ub}|. \quad (\text{B9})$$

As a final comment, we note that in principle one could add a complete set of VL partners $U_{L,R}, N_{L,R}, D_{L,R}, E_{L,R}$ with the same quantum numbers as their corresponding light family RH fields. In this case, another interesting limit is that of large mixing (small cosine $c_{D,E}$) for the down-type partners, which could be exploited to explain the smallness of the down-type Yukawas while simultaneously reducing the magnitude of RH currents in the down-sector.

Appendix C: Expressions for $R_{D(*)}$

Defining $\delta R_{D(*)} = R_{D(*)}/R_{D(*)}^{\text{SM}} - 1$, we have

$$\delta R_D \approx 2 \text{Re} \left\{ C_U \beta_L^{b\tau} \left[\rho_{LL,33}^{\text{NLO}} \beta_L^{b\tau*} \left(1 + \frac{\rho_{LL,23}^{\text{NLO}}}{\rho_{LL,33}^{\text{NLO}}} A \right) - 1.50 \eta_s \rho_{LR,33}^{\text{NLO}} \beta_R^{b\tau*} \left(1 + \frac{\rho_{LR,23}^{\text{NLO}}}{\rho_{LR,33}^{\text{NLO}}} A \right) \right] \right\}, \quad (\text{C1})$$

$$\delta R_{D^*} \approx 2 \text{Re} \left\{ C_U \beta_L^{b\tau} \left[\rho_{LL,33}^{\text{NLO}} \beta_L^{b\tau*} \left(1 + \frac{\rho_{LL,23}^{\text{NLO}}}{\rho_{LL,33}^{\text{NLO}}} A \right) - 0.12 \eta_s \rho_{LR,33}^{\text{NLO}} \beta_R^{b\tau*} \left(1 + \frac{\rho_{LR,23}^{\text{NLO}}}{\rho_{LR,33}^{\text{NLO}}} A \right) \right] \right\}, \quad (\text{C2})$$

where $\eta_s = 1.7$ and

$$A = \left(\frac{V_{cs}}{V_{cb}} \frac{\beta_L^{s\tau}}{\beta_L^{b\tau}} + \frac{V_{cd}}{V_{cb}} \frac{\beta_L^{d\tau}}{\beta_L^{b\tau}} \right). \quad (\text{C3})$$

The NLO corrections to \mathcal{O}_{LL}^U and \mathcal{O}_{LR}^U contributing to $b \rightarrow c \tau \nu$ transitions read [25]

$$\rho_{LL,33}^{\text{NLO}} = 1 + \frac{\alpha_4}{4\pi} \left(\frac{17}{12} f_1(x_{Z'}) + \frac{4}{3} f_1(x_{G'}) \right), \quad (\text{C4})$$

$$\rho_{LL,23}^{\text{NLO}} = 1 + \frac{\alpha_4}{4\pi} \left(\frac{7}{8} f_1(x_{Z'}) + \left(\frac{13}{24} f_2(x_{Z'}, x_Q) + \frac{4}{3} f_2(x_{G'}, x_Q) \right) c_q^2 \right), \quad (\text{C5})$$

$$\rho_{LR,33}^{\text{NLO}} = 1 + \frac{\alpha_4}{4\pi} \left(\frac{23}{12} f_1(x_{Z'}) + \frac{16}{3} f_1(x_{G'}) \right), \quad (\text{C6})$$

$$\rho_{LR,23}^{\text{NLO}} = 1 + \frac{\alpha_4}{4\pi} \left(\frac{13}{8} f_1(x_{Z'}) + \left(\frac{7}{24} f_2(x_{Z'}, x_Q) + \frac{16}{3} f_2(x_{G'}, x_Q) \right) c_q^2 \right), \quad (\text{C7})$$

with $x_Q = m_Q^2/m_U^2$ and

$$f_1(x_V) = \frac{\log(x_V)}{x_V - 1}, \quad (\text{C8})$$

$$f_2(x_V, x_Q) = \frac{1}{x_V - x_Q} \left(\frac{x_V \log(x_V)}{x_V - 1} - \frac{x_Q \log(x_Q)}{x_Q - 1} \right). \quad (\text{C9})$$

Appendix D: Wilson coefficients

In Table II we report the Wilson coefficients of operators contributing to $\Delta Q = 2$ and $K \rightarrow \pi \nu \bar{\nu}$ transitions, as normalized in (20) and (42).

Wilson coefficient	Tree level		Box diagrams	Flavor changing vertices	
	G'	Z'	$[U_1 \ U_1]$	G'	Z'
\mathcal{C}_{qq}^{3333}	$\frac{1}{3x_{G'}}$	$\frac{1}{24x_{Z'}}$	$\frac{g_4^2}{32\pi^2} B_{qq}^{1111}$	0	0
\mathcal{C}_{qq}^{2333}	0	0	$-\frac{g_4^2}{32\pi^2} s_q B_{qq}^{1211}$	$\frac{g_4^2}{32\pi^2} \beta_{bL}^* \beta_{sL} \frac{V_{G'}}{3x_{G'}}$	$\frac{g_4^2}{32\pi^2} \beta_{bL}^* \beta_{sL} \frac{V_{Z'_q}}{24x_{Z'}}$
\mathcal{C}_{qq}^{3233}	0	0	$-\frac{g_4^2}{32\pi^2} s_q B_{qq}^{2111}$	$\frac{g_4^2}{32\pi^2} \beta_{bL} \beta_{sL}^* \frac{V_{G'}}{3x_{G'}}$	$\frac{g_4^2}{32\pi^2} \beta_{bL} \beta_{sL}^* \frac{V_{Z'_q}}{24x_{Z'}}$
\mathcal{C}_{qq}^{2233}	$\frac{(\epsilon_3 - s_q^2)}{6x_{G'}}$	$-\frac{(\epsilon_1 - s_q^2)}{24x_{Z'}}$	$\frac{g_4^2}{32\pi^2} s_q^2 B_{qq}^{2211}$	0	0
\mathcal{C}_{qq}^{2332}	$-\frac{(\epsilon_3 - s_q^2)}{2x_{G'}}$	0	$\frac{g_4^2}{32\pi^2} s_q^2 B_{qq}^{1212}$	0	0
\mathcal{C}_{qq}^{2323}	0	0	$\frac{g_4^2}{32\pi^2} s_q^2 B_{qq}^{1221}$	0	0
\mathcal{C}_{qq}^{3232}	0	0	$\frac{g_4^2}{32\pi^2} s_q^2 B_{qq}^{2112}$	0	0
\mathcal{C}_{qq}^{2223}	0	0	$-\frac{g_4^2}{32\pi^2} s_q^3 B_{qq}^{2221}$	$-\frac{g_4^2}{32\pi^2} (\epsilon_3 - s_q^2) \beta_{bL}^* \beta_{sL} \frac{V_{G'}}{3x_{G'}}$	$-\frac{g_4^2}{32\pi^2} (\epsilon_1 - s_q^2) \beta_{bL}^* \beta_{sL} \frac{V_{Z'_q}}{24x_{Z'}}$
\mathcal{C}_{qq}^{2232}	0	0	$-\frac{g_4^2}{32\pi^2} s_q^3 B_{qq}^{2212}$	$-\frac{g_4^2}{32\pi^2} (\epsilon_3 - s_q^2) \beta_{bL} \beta_{sL}^* \frac{V_{G'}}{3x_{G'}}$	$-\frac{g_4^2}{32\pi^2} (\epsilon_1 - s_q^2) \beta_{bL} \beta_{sL}^* \frac{V_{Z'_q}}{24x_{Z'}}$
\mathcal{C}_{qq}^{2222}	$\frac{(\epsilon_3 - s_q^2)^2}{3x_{G'}}$	$\frac{(\epsilon_1 - s_q^2)^2}{24x_{Z'}}$	$\frac{g_4^2}{32\pi^2} s_q^4 B_{qq}^{2222}$	0	0
\mathcal{C}_{qq}^{1133}	$\frac{\epsilon_3}{6x_{G'}}$	$-\frac{\epsilon_1}{24x_{Z'}}$	0	0	0
\mathcal{C}_{qq}^{1331}	$-\frac{\epsilon_3}{2x_{G'}}$	$-\frac{\epsilon_1}{24x_{Z'}}$	0	0	0
\mathcal{C}_{qq}^{1123}	0	0	0	$\epsilon_3 \frac{g_4^2}{32\pi^2} \beta_{bL}^* \beta_{sL} \frac{V_{G'}}{6x_{G'}}$	$-\epsilon_1 \frac{g_4^2}{32\pi^2} \beta_{bL}^* \beta_{sL} \frac{V_{Z'_q}}{24x_{Z'}}$
\mathcal{C}_{qq}^{1321}	0	0	0	$-\epsilon_3 \frac{g_4^2}{32\pi^2} \beta_{bL}^* \beta_{sL} \frac{V_{G'}}{2x_{G'}}$	0
\mathcal{C}_{qq}^{1132}	0	0	0	$\epsilon_3 \frac{g_4^2}{32\pi^2} \beta_{bL} \beta_{sL}^* \frac{V_{G'}}{6x_{G'}}$	$-\epsilon_1 \frac{g_4^2}{32\pi^2} \beta_{bL} \beta_{sL}^* \frac{V_{Z'_q}}{24x_{Z'}}$
\mathcal{C}_{qq}^{1231}	0	0	0	$-\epsilon_3 \frac{g_4^2}{32\pi^2} \beta_{bL}^* \beta_{sL} \frac{V_{G'}}{2x_{G'}}$	0
\mathcal{C}_{qq}^{1122}	$-\frac{\epsilon_3(\epsilon_3 - s_q^2)}{6x_{G'}}$	$\frac{\epsilon_1(\epsilon_1 - s_q^2)}{24x_{Z'}}$	0	0	0
\mathcal{C}_{qq}^{1221}	$\frac{\epsilon_3(\epsilon_3 - s_q^2)}{2x_{G'}}$	$\frac{\epsilon_1(\epsilon_1 - s_q^2)}{24x_{Z'}}$	0	0	0
\mathcal{C}_{qq}^{1111}	$\frac{\epsilon_3^2}{3x_{G'}}$	$\frac{\epsilon_1^2}{24x_{Z'}}$	0	0	0
$\mathcal{C}_{\ell q}^{3333}$	0	$-\frac{1}{4x_{Z'}}$	$-\frac{g_4^2}{16\pi^2} B_{q\ell}^{1111}$	0	0
$\mathcal{C}_{\ell q}^{3332}$	0	0	$\frac{g_4^2}{16\pi^2} s_q B_{q\ell}^{2111}$	0	$-\frac{g_4^2}{16\pi^2} \beta_{bL} \beta_{sL}^* \frac{V_{Z'_q}}{8x_{Z'}}$
$\mathcal{C}_{\ell q}^{3323}$	0	0	$\frac{g_4^2}{16\pi^2} s_q B_{q\ell}^{1211}$	0	$-\frac{g_4^2}{16\pi^2} \beta_{bL}^* \beta_{sL} \frac{V_{Z'_q}}{8x_{Z'}}$
$\mathcal{C}_{\ell q}^{3322}$	0	$\frac{(\epsilon_1 - s_q^2)}{4x_{Z'}}$	$-\frac{g_4^2}{16\pi^2} s_q^2 B_{q\ell}^{2211}$	0	0
$\mathcal{C}_{\ell q}^{3311}$	0	$\frac{\epsilon_1}{4x_{Z'}}$	0	0	0

TABLE II. Coefficients of the effective operators, normalized as in (20) and (42), at tree level and next-to-leading order. The loop functions $B_{qq}^{ijkl} \equiv B_{qq}^{ijkl}(x_L, x_Q)$, $B_{\ell q}^{ij\alpha\beta} \equiv B_{\ell q}^{ij\alpha\beta}(x_L, x_Q)$, $V_{G'} \equiv V_{G'}(x_L)$, and $V_{Z'_q} \equiv V_{Z'_q}(x_L)$, where $x_{Q,L} = m_{Q,L}^2/m_{U_1}^2$, can be found in [26]. Note that $C_{qq}^{ijkl} = C_{qq}^{klji}$.

-
- [1] LHCb collaboration, R. Aaij et al., *Test of lepton universality using $B^+ \rightarrow K^+ \ell^+ \ell^-$ decays*, *Phys. Rev. Lett.* **113** (2014) 151601, [1406.6482].
- [2] LHCb collaboration, R. Aaij et al., *Test of lepton universality with $B^0 \rightarrow K^{*0} \ell^+ \ell^-$ decays*, *JHEP* **08** (2017) 055, [1705.05802].
- [3] LHCb collaboration, R. Aaij et al., *Search for lepton-universality violation in $B^+ \rightarrow K^+ \ell^+ \ell^-$ decays*, *Phys. Rev. Lett.* **122** (2019) 191801, [1903.09252].
- [4] LHCb collaboration, R. Aaij et al., *Test of lepton universality in beauty-quark decays*, *Nature Phys.* **18** (2022) 277–282, [2103.11769].
- [5] BABAR collaboration, J. P. Lees et al., *Evidence for an excess of $\bar{B} \rightarrow D^{(*)} \tau^- \bar{\nu}_\tau$ decays*, *Phys. Rev. Lett.* **109** (2012) 101802, [1205.5442].
- [6] BABAR collaboration, J. P. Lees et al., *Measurement of*

- an Excess of $\bar{B} \rightarrow D^{(*)}\tau^-\bar{\nu}_\tau$ Decays and Implications for Charged Higgs Bosons, *Phys. Rev. D* **88** (2013) 072012, [1303.0571].
- [7] BELLE collaboration, M. Huschle et al., Measurement of the branching ratio of $\bar{B} \rightarrow D^{(*)}\tau^-\bar{\nu}_\tau$ relative to $\bar{B} \rightarrow D^{(*)}\ell^-\bar{\nu}_\ell$ decays with hadronic tagging at Belle, *Phys. Rev. D* **92** (2015) 072014, [1507.03233].
- [8] LHCb collaboration, R. Aaij et al., Measurement of the ratio of branching fractions $\mathcal{B}(\bar{B}^0 \rightarrow D^{*+}\tau^-\bar{\nu}_\tau)/\mathcal{B}(\bar{B}^0 \rightarrow D^{*+}\mu^-\bar{\nu}_\mu)$, *Phys. Rev. Lett.* **115** (2015) 111803, [1506.08614].
- [9] LHCb collaboration, R. Aaij et al., Measurement of the ratio of the $B^0 \rightarrow D^{*-}\tau^+\nu_\tau$ and $B^0 \rightarrow D^{*-}\mu^+\nu_\mu$ branching fractions using three-prong τ -lepton decays, *Phys. Rev. Lett.* **120** (2018) 171802, [1708.08856].
- [10] LHCb collaboration, R. Aaij et al., Test of Lepton Flavor Universality by the measurement of the $B^0 \rightarrow D^{*-}\tau^+\nu_\tau$ branching fraction using three-prong τ decays, *Phys. Rev. D* **97** (2018) 072013, [1711.02505].
- [11] A. J. Buras, D. Buttazzo, J. Girrbach-Noe and R. Kneijens, $K^+ \rightarrow \pi^+\nu\bar{\nu}$ and $K_L \rightarrow \pi^0\nu\bar{\nu}$ in the Standard Model: status and perspectives, *JHEP* **11** (2015) 033, [1503.02693].
- [12] NA62 collaboration, E. Cortina Gil et al., Measurement of the very rare $K^+ \rightarrow \pi^+\nu\bar{\nu}$ decay, *JHEP* **06** (2021) 093, [2103.15389].
- [13] M. Bordone, D. Buttazzo, G. Isidori and J. Monnard, Probing Lepton Flavour Universality with $K \rightarrow \pi\nu\bar{\nu}$ decays, *Eur. Phys. J. C* **77** (2017) 618, [1705.10729].
- [14] S. Descotes-Genon, S. Fajfer, J. F. Kamenik and M. Novoa-Brunet, Implications of $b \rightarrow s\mu\mu$ anomalies for future measurements of $B \rightarrow K^{(*)}\nu\bar{\nu}$ and $K \rightarrow \pi\nu\bar{\nu}$, *Phys. Lett. B* **809** (2020) 135769, [2005.03734].
- [15] S. Fajfer, N. Košnik and L. Vale Silva, Footprints of leptquarks: from $R_{K^{(*)}}$ to $K \rightarrow \pi\nu\bar{\nu}$, *Eur. Phys. J. C* **78** (2018) 275, [1802.00786].
- [16] D. Marzocca, S. Trifinopoulos and E. Venturini, From B -meson anomalies to Kaon physics with scalar leptquarks, *Eur. Phys. J. C* **82** (2022) 320, [2106.15630].
- [17] R. Alonso, B. Grinstein and J. Martin Camalich, Lepton universality violation and lepton flavor conservation in B -meson decays, *JHEP* **10** (2015) 184, [1505.05164].
- [18] L. Calibbi, A. Crivellin and T. Ota, Effective Field Theory Approach to $b \rightarrow s\ell\ell^{(\prime)}$, $B \rightarrow K^{(*)}\nu\bar{\nu}$ and $B \rightarrow D^{(*)}\tau\nu$ with Third Generation Couplings, *Phys. Rev. Lett.* **115** (2015) 181801, [1506.02661].
- [19] R. Barbieri, G. Isidori, A. Pattori and F. Senia, Anomalies in B -decays and $U(2)$ flavour symmetry, *Eur. Phys. J. C* **76** (2016) 67, [1512.01560].
- [20] B. Bhattacharya, A. Datta, J.-P. Guévin, D. London and R. Watanabe, Simultaneous Explanation of the R_K and $R_{D^{(*)}}$ Puzzles: a Model Analysis, *JHEP* **01** (2017) 015, [1609.09078].
- [21] D. Buttazzo, A. Greljo, G. Isidori and D. Marzocca, B -physics anomalies: a guide to combined explanations, *JHEP* **11** (2017) 044, [1706.07808].
- [22] L. Di Luzio, A. Greljo and M. Nardecchia, Gauge leptquark as the origin of B -physics anomalies, *Phys. Rev. D* **96** (2017) 115011, [1708.08450].
- [23] M. Bordone, C. Cornella, J. Fuentes-Martin and G. Isidori, A three-site gauge model for flavor hierarchies and flavor anomalies, *Phys. Lett. B* **779** (2018) 317–323, [1712.01368].
- [24] A. Greljo and B. A. Stefanek, Third family quark–lepton unification at the TeV scale, *Phys. Lett. B* **782** (2018) 131–138, [1802.04274].
- [25] J. Fuentes-Martín, G. Isidori, M. König and N. Selimović, Vector Leptoquarks Beyond Tree Level, *Phys. Rev. D* **101** (2020) 035024, [1910.13474].
- [26] J. Fuentes-Martín, G. Isidori, M. König and N. Selimović, Vector Leptoquarks Beyond Tree Level III: Vector-like Fermions and Flavor-Changing Transitions, *Phys. Rev. D* **102** (2020) 115015, [2009.11296].
- [27] J. C. Pati and A. Salam, Lepton Number as the Fourth Color, *Phys. Rev. D* **10** (1974) 275–289.
- [28] J. Fuentes-Martin, G. Isidori, J. M. Lizana, N. Selimovic and B. A. Stefanek, Flavor hierarchies, flavor anomalies, and Higgs mass from a warped extra dimension, **2203.01952**.
- [29] J. Fuentes-Martin, G. Isidori, J. Pagès and B. A. Stefanek, Flavor non-universal Pati-Salam unification and neutrino masses, *Phys. Lett. B* **820** (2021) 136484, [2012.10492].
- [30] G. Panico and A. Pomarol, Flavor hierarchies from dynamical scales, *JHEP* **07** (2016) 097, [1603.06609].
- [31] L. Allwicher, G. Isidori and A. E. Thomsen, Stability of the Higgs Sector in a Flavor-Inspired Multi-Scale Model, *JHEP* **01** (2021) 191, [2011.01946].
- [32] R. Barbieri, A View of Flavour Physics in 2021, *Acta Phys. Polon. B* **52** (2021) 789, [2103.15635].
- [33] R. Barbieri and A. Tesi, B -decay anomalies in Pati-Salam $SU(4)$, *Eur. Phys. J. C* **78** (2018) 193, [1712.06844].
- [34] J. Fuentes-Martín and P. Stangl, Third-family quark-lepton unification with a fundamental composite Higgs, *Phys. Lett. B* **811** (2020) 135953, [2004.11376].
- [35] C. Cornella, J. Fuentes-Martin and G. Isidori, Revisiting the vector leptoquark explanation of the B -physics anomalies, *JHEP* **07** (2019) 168, [1903.11517].
- [36] L. Di Luzio, J. Fuentes-Martin, A. Greljo, M. Nardecchia and S. Renner, Maximal Flavour Violation: a Cabibbo mechanism for leptoquarks, *JHEP* **11** (2018) 081, [1808.00942].
- [37] C. Cornella, D. A. Faroughy, J. Fuentes-Martin, G. Isidori and M. Neubert, Reading the footprints of the B -meson flavor anomalies, *JHEP* **08** (2021) 050, [2103.16558].
- [38] “Flavor constraints on new physics.” <https://agenda.infn.it/event/14377/contributions/24434/attachments/17481/19830/silvestriniLaThuile.pdf>.
- [39] UFIT collaboration, M. Bona et al., Model-independent constraints on $\Delta F = 2$ operators and the scale of new physics, *JHEP* **03** (2008) 049, [0707.0636].
- [40] A. J. Buras, S. Jager and J. Urban, Master formulae for $\Delta F=2$ NLO QCD factors in the standard model and beyond, *Nucl. Phys. B* **605** (2001) 600–624, [hep-ph/0102316].
- [41] G. Buchalla and A. J. Buras, The rare decays $K \rightarrow \pi\nu\bar{\nu}$, $B \rightarrow X\nu\bar{\nu}$ and $B \rightarrow l^+l^-$: An Update, *Nucl. Phys. B* **548** (1999) 309–327, [hep-ph/9901288].
- [42] A. Celis, J. Fuentes-Martin, A. Vicente and J. Virto, *DsixTools: The Standard Model Effective Field Theory Toolkit*, *Eur. Phys. J. C* **77** (2017) 405, [1704.04504].